Journal of Naval Architecture and Marine Engineering
December, 2023
http://dx.doi.org/10.3329/jname.v20i3.70115 *http://www.banglajol.info*

NUMERICAL ANALYSIS OF FLOW OVER BLUFF BODIES WITH DIFFERENT SHAPES

A. M. Abir[1], P. R. Chowdhury[2*] and G. K. Saha[3]

[1]Department of Naval Architecture and Marine Engineering, Bangladesh University of Engineering and Technology, Dhaka, Bangladesh, adnanmasruf1998@gmail.com
[2]Department of Naval Architecture and Marine Engineering, Bangladesh University of Engineering and Technology, Dhaka, Bangladesh, paramaroy@name.buet.ac.bd
[3]Department of Naval Architecture and Marine Engineering, Bangladesh University of Engineering and Technology, Dhaka, Bangladesh, goutamkumar@name.buet.ac.bd

Abstract:

In this study, Ansys Fluent solver with SIMPLE algorithm and K-Epsilon turbulence model is used to determine the drag forces on bluff bodies with different shapes and arrangements at different Reynolds numbers. In the process, the cross-sectional areas of all the bodies are kept approximately the same to keep the amount of material same for all the cases. First, simulations of the 2D unsteady viscous flow around cylinders of circular and elliptical shapes with the same cross-sectional area are performed at Reynolds number 1000. In the case of elliptical cylinder, two different orientations are used, namely: major axis along the flow (horizontal orientation) and major axis perpendicular to the flow (vertical orientation) for aspect ratio of 0.8. The horizontally oriented elliptical cylinder shows the least drag compared to the circular and vertically oriented elliptical cylinders. The vertically oriented elliptical cylinder shows the maximum drag because of the large projected area and early flow separation from the cylinder. Later, the drag coefficients of two circular cylinders of the same diameter in tandem arrangement are investigated at inlet speeds of 2.5, 5, 7.5, and 10.5 knots considering L/D ratios of 2.0, 2.5, and 3.0, where L is the center-to-center distance and D is the diameter of the cylinders. For the upstream(first) cylinder, the flow separation from the cylinder is delayed as the speed increases, and the wake becomes narrower. Consequently, the drag coefficient for the first cylinder decreases with increase in speed. As the speed increases, the disturbance on the downstream(second) cylinder increases with respect to the first cylinder, and hence the drag coefficient increases.

Keywords: Two-dimensional bluff bodies, circular cylinder, elliptical cylinder, tandem arrangement, CFD, K-Epsilon turbulence model.

NOMENCLATURE

σ_k	Prandtl number for turbulent kinetic energy	k	turbulent kinetic energy
σ_ε	Prandtl number for turbulent dissipation	U	velocity vector
ρ	water density	p	pressure
ε	turbulent dissipation rate	P_k	production due to mean velocity shear
μ_t	turbulent viscosity	P_b	production due to buoyancy
μ	dynamic viscosity	S_k, S_ε	user defined source terms

1. Introduction

Flow around single bluff bodies and multiple cylinders in tandem has been a topic of interest for researchers for many years. Specially flow around a pair of cylinders in different arrangement has intrigued many researchers over time. This is not only because understanding the flow around two circular cylinders is fundamental to understanding the flow around multiple cylinders in complex arrangements, but because the flow interference between the two circular cylinders causes a wake-induced vibration (Bokaian and Geoola,1984).). have identified three distinctive arrangements of cylinders, namely: Tandem arrangement, Side by side arrangement, Staggered arrangement. The drag force acting on circular cylinders in tandem arrangement changes with the spacing ratio (center-to-center distance of the cylinders and their significant length: in the case of circular cylinder, the diameter), Reynolds number, and angle of attack (Zdravkovich, 1977)). We are interested in tandem arrangement

1813-8535 (Print), 2070-8998 (Online) Selected from papers presented at MARTEC2022.

in this study. There is a sudden jump in combined drag force between the spacing of 3D to 4D for Re = 9.72×10^3 in the case of flow around two circular wires of diameter 12.5 mm in tandem arrangement (Pannell et al ,1915). For Re = 1.63×10^5, 1.14×10^5,0.65×10^5 the C_d of the upstream cylinder decreases up to spacing ratio of 3.5 and then increases and reaches a steady value. For the downstream cylinder, C_d increases up to a spacing of 2.5D and then decreases up to 3.5D and finally increases to a steady value for greater spacing (Biermann and Herrnstein, 1933). No vortex shedding is detected behind the upstream cylinder until the spacing ratio reaches 3.8. However, vortex shedding is observed for the downstream cylinder at all spacings (Oka et al, 1972). At 1.0< L/D<3.8, the upstream cylinder produces no vortex shedding and thus less prone to vibration. But downstream cylinder always produces vortex shedding and is thus more prone to vortex shedding compared to single cylinder. At L/D >3.8, both cylinders are prone to vortex shedding (King and Johns, 1976). So, the flow patterns, drag forces and vortex shedding pattern change at a certain spacing in the case of tandem arrangement. This is called the critical spacing (Ishigai et al, 1972). Numerical studies of two cylinders arranged in tandem have also backed up the trend of initial decrease of drag coefficient of the upstream cylinder and then a jump in drag coefficient at critical spacing at various Reynolds numbers both for 2D and 3D analysis (Kitagawa and Ohta, 2008 and Hu et al, 2019). For Re < = 2.5×10^5, the critical spacing is at L/D = 3.8 (Okajima, 1979). The critical spacing is at L/D = 3.5 for Re in the order of 1×10^4 (Igarashi, 1981). At Re = 2×10^4 the critical spacing decreased from L/D = 3.5 to L/D = 2.5 as the turbulence intensity grew from 0.1% to 1.4% (Ljungkrona et al,1991). Two-cylinder flow is more sensitive to Re than single cylinder flow (Derakhshandeh and Alam, 2020). Achenbach (1968), termed Reynolds number greater than 1.5×10^6 as super critical Reynolds number. As can be seen from the preceding discussion, a few studies on the hydrodynamic properties of tandem cylinders at supercritical Reynolds numbers have been conducted. For this reason, the drag coefficient for Reynolds numbers ranging from 1.28×10^6 to 5.5×10^6 for spacing ratio 2, 2.5 and 3 has been calculated in this study to see the pattern of drag coefficient with speed. The speed range of the water flow is selected based on the seasonal variations in speed in the rivers, like The Padma. In the year 2005, the river Padma's greatest flow speed was measured at 4.85 m/s near Baruria Transit (Mahmud et al, 2018). Depending on the data from the literature, the speed range is selected from 2.5 knots to 10.5 knots, or 1.28 to 5.41 m/s. Bangladesh has very well-articulated inland and maritime waterways. Quite recently, Bangladesh has built the Padma Bridge on one of the prominent inland waterways, the Padma River. The Padma River has one of the strongest currents in the world. The interaction of flow with the supporting columns of the bridge exerts drag force and moments on the columns. Besides, erosion of the column surface takes place due to the forces on the columns. These forces and moments depend on the gap between the columns and the flow interference due to the orientation of the columns. By numerically calculating the drag force on tandem cylinders, it is possible to predict the force experienced by such structures prior to their construction. This can help reduce the forces on structures by taking necessary actions. Based on the studies on cylinders and the review of the literature, the following are the objectives of this study:

- To compare the drag coefficients between circular and elliptical cylinders with the same cross-sectional area and at the same Reynolds number.
- To present the drag coefficient vs flow speed at different spacing ratios for two circular cylinders in tandem arrangement.

2. Mathematical Formulation

In fluid dynamics, the main governing equations of the fluid are Navier-Stokes equations. Navier-Stokes equation is based on the physical property conservation law for fluids. The conservational law states that the input and output determine the change of properties of an object, such as mass, energy, and momentum. The Navier-Stokes equations consists of a time-dependent continuity equation for conservation of mass, three time-dependent conservation of momentum equations and a time-dependent conservation of energy equation. The conservation equations of fluid mass and momentum for a steady, incompressible, and viscous flow are:

$$\vec{\nabla}.\vec{U} = 0 \tag{1}$$

$$\rho \frac{DU}{Dt} = -\nabla p + \mu\nabla^2(U) + \rho.g \tag{2}$$

In the RANS model, each and all terms in the Navier Stokes equation are time averaged to get an overall view of the flow. The k-epsilon model for turbulence belongs to the RANS model family. It is a two-equation model.

Apart from the conservation equations, it solves two extra transport equations for turbulent kinetic energy (k) and turbulent dissipation rate (epsilon- ε), which determine the dissipation rate of turbulent kinetic energy. Here the k-epsilon standard equation is used. The corresponding equations are:

$$k = \frac{\partial(\rho \kappa)}{\partial t} + \nabla.(\rho U \mathrm{k}) = \nabla.[(\mu + \frac{\mu_t}{\sigma_k})\nabla k] + P_k + P_b - \rho\varepsilon + S_k \quad (3)$$

$$\varepsilon = \frac{\partial(\rho\varepsilon)}{\partial t} + \nabla.(\rho U\varepsilon) = \nabla.[\left(\mu + \frac{\mu_t}{\sigma_\varepsilon}\right)\nabla\varepsilon] + \frac{C_1\varepsilon}{k}(P_k + C_3P_b) - \frac{C_2\rho\varepsilon^2}{k} + S_\varepsilon \quad (4)$$

3. Case Study and Models

In this paper, four case studies have been investigated. The studies of single circular, elliptical, and aerofoil shaped cylinders are done at Re = 1000 for comparison of the drag coefficients. The study of two circular cylinders in tandem arrangement has been done at flow speeds ranging from 2.5 to 10.5 knots.

3.1 Single circular cylinder

The detailed geometry and domain specifications of a single circular cylinder are given in Table 1 and Figure 1.

Table 1. Specifications of single circular cylinder

Circular Cylinder	
Diameter D (m)	1.000
Reynolds number (Re)	1000

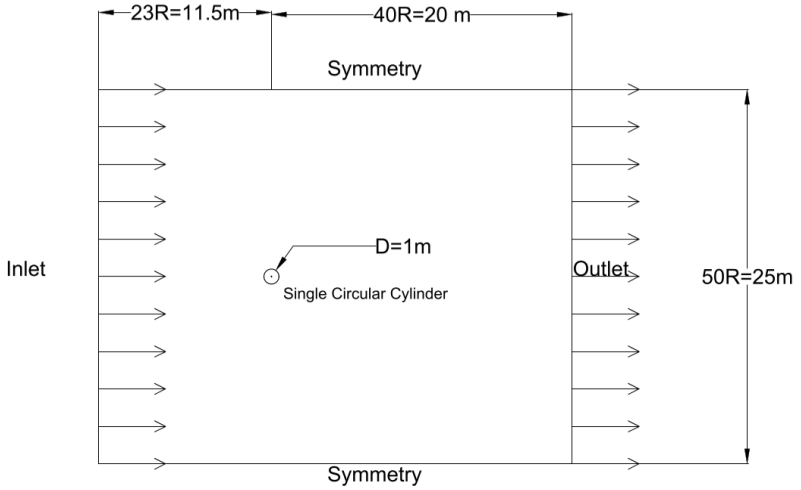

Fig. 1: Domain of single circular cylinder

The mesh is a structured mesh with number of cells 37860.

3.2 Two circular cylinders in tandem arrangement

Two circular cylinders of equal diameter have been analyzed at three different spacings of L/D = 2.0, 2.5, and 3.0. Here L is the center-to-center distance of the two cylinders, and D is the diameter (see Figure 2). The inlet speeds of water flow varied from 2.5 to 10.5 knots at each spacing ratio. The specifications are given below in Table 2 for two circular cylinders in tandem arrangement at different spacing ratios.

Table 2. Tandem arrangement specification

Tandem arrangement of circular cylinders	
Diameter(m)	1.000
Length to Diameter ratio, L/D	2.0, 2.5 and 3.0
Inlet speeds(knots) at each spacing ratio	2.5, 5.0, 7.5 and 10.5

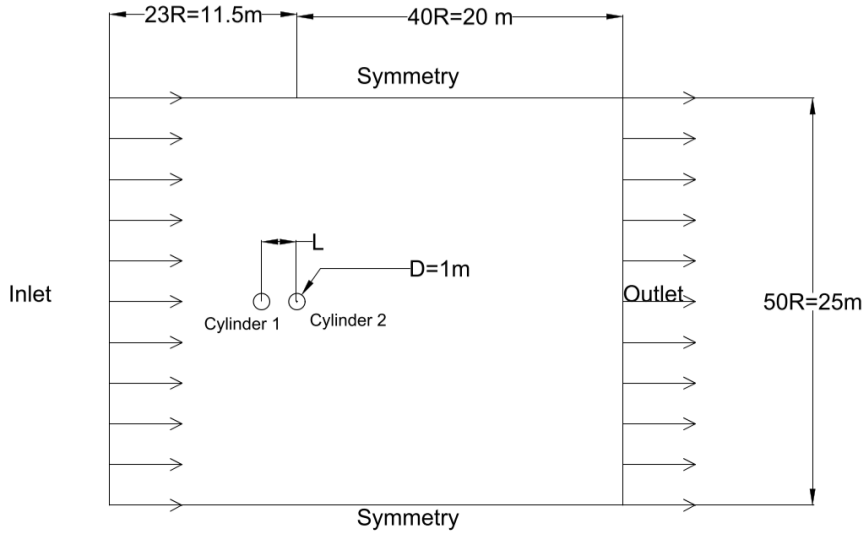

Fig. 2: Domain of tandem arrangement

The number of cells in the structured mesh for L/D = 2.0, 2.5 and 3.0 are 176000, 182800 and 187900 respectively.

3.3 Elliptical cylinder

Elliptical cylinders have been used in two different orientations. One has the major axis along the flow (horizontal orientation), and the other has the major axis perpendicular to the flow (vertical orientation). See Table 3 and Figure 3 for details. The mesh is structured with 37,500 cells.

Table 3. Specifications of elliptical cylinder

Elliptical Cylinder	
Major axis length 2a (m)	1.118
Minor axis Length 2b (m)	0.8944
Aspect ratio(b/a)	0.8
Reynolds number	1000

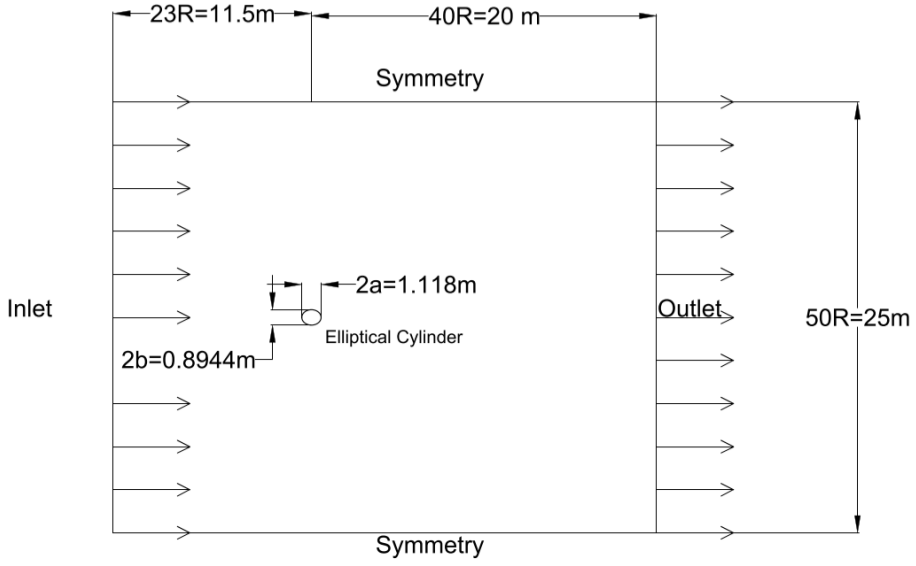

Fig. 3: Domain of elliptical cylinder

In Figure 3, only horizontal orientation is shown. Later, the same cylinder is oriented vertically.

3.4 Streamline body-NACA 0012

This shape is used particularly to compare the drag coefficients between bluff body and streamline body. The specifications and geometry are placed in Table 4 and Figure 4.

Table 4. Specifications of NACA 0012

NACA 0012	
Chord (m)	0.95
Reynolds number	1000

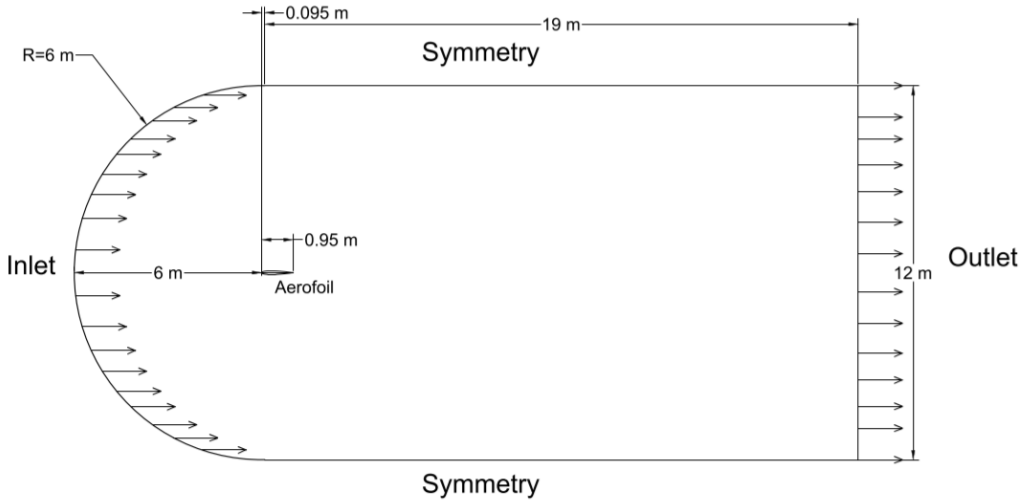

Fig. 4: Domain of NACA 0012

The domain is discretized with a structured mesh with number of cells 10020.

3.5 Model setup

k- ε turbulence modelling with standard wall function in the near wall treatment has been used to handle turbulence. The boundary conditions are a velocity boundary condition at the inlet, constant pressure at the outlet, and symmetry at the other two slides of the flow domain. The SIMPLE scheme is used to solve the pressure-velocity coupling. A time step size of 0.05 second and 2000 iterations per time step are employed for all the cases to solve the solutions iteratively. All the analyses are pressure-based, and the equations of pressure are second order.

4. Validation

In any numerical investigation, establishing grid convergence is a must. It is critical to ensure that the equations are accurately solved, and that the solution is unaffected by grid resolution. To check the grid convergence, at least three simulations are completed (coarse, medium, fine) with a constant refinement ratio, r. A parameter indicative of grid convergence is chosen. In this study, drag coefficient is chosen. The order of convergence, P is calculated using the following equation.

$$P = \ln\left(\frac{(f_3 - f_2)}{(f_2 - f_1)}\right) / \ln(r) \tag{5}$$

f_1 to f_3 are the results from each grid level (from fine to coarse). Richardson extrapolation

$$C_{d,h=0} = f_{fine} + \frac{(f_1 - f_2)}{r^p - 1} \tag{6}$$

is performed, to predict the value at h = 0 where h = 0 means the theoretical finest normalized grid spacing. Grid convergence index (GCI) for the medium and fine refinement levels is calculated as

$$GCI = \frac{F_{a|e|}}{r^p - 1} \tag{7}$$

where e is the error between the two grids and F_a is the safety factor. Generally, the safety factor is taken as 2. Grids are in the asymptotic range of convergence if asymptotic relationship.

$$\frac{GCI_{2-3}}{r^p \times GCI_{1-2}} \approx 1 \tag{8}$$

For the single circular cylinder, three grids are generated, and the sizes are shown in Table 5.

Table 5. Different grid sizes for single circular cylinder

Grid	Size	Drag Coefficient
Fine (1)	256×255	0.933
Medium (2)	180×180	0.937
Coarse (3)	129×128	0.943

Here, the ratio between the sizes of coarse to medium and medium to fine meshes ≈ $\sqrt{2}$. Hence r = $\sqrt{2}$.Using the values, P=1.32, $C_{d,h=0} = 0.927$, GCI_{2-3}=2.14%, GCI_{1-2}=1.36%. Finally, the asymptotic range of convergence $\frac{GCI_{2-3}}{r^p \times GCI_{1-2}} = \frac{2.14\%}{\sqrt{2}^{1.32} \times 1.36\%}$ =0. 995≈1.Hence, grid convergence for the single circular cylinder is achieved in the given domain. The medium grid is chosen for saving computational time. To compare the result of single circular cylinder with literature, a comparison in Table 6 is shown. The value of Drag coefficient for single cylinder is found to be 0.937 at Re = 1000 closer to Rahman et. al. (2007) where C_d is 0.995.

Table 6. Comparison of drag coefficient with literature

Drag Coefficient in Present Study	0.937
Rahman et al. (2007)	0.995
% Deviation from literature	5.83%

5. Results and Discussion

The drag coefficients for the single circular, elliptical and aerofoil shapes are given in the Table 7.

Table 7. Comparison of drag coefficients

Drag Coefficients at Re = 1000			
Circular	**Elliptical -Horizontal**	**Elliptical -Vertical**	**Aerofoil**
0.937	0.813	1.142	0.206

Various studies have shown that pressure drag dominates drag force on bluff bodies. This pressure drag is dependent on the shape and orientation of the body. The elliptical cylinder in the vertical orientation has the maximum drag coefficient because the flow separates early from it compared to others, resulting in a wider wake size. The pressure loss is higher in the wake. This results in an increase in the pressure difference between the front and rear of the cylinder. Thus, the drag coefficient rises. The drag coefficient decreases as we move from the circular cylinder to the elliptical cylinder in horizontal orientation. The wake size of the horizontal elliptical cylinder is less than that of the circular cylinder. Thus, the pressure loss at the wake is smaller for the elliptical cylinder in horizontal orientation. This results in a lower drag coefficient. The aerofoil shape is used to compare the drag coefficients between bluff bodies and streamline bodies. In a streamlined body, pressure drag is insignificant, and the drag force is dominated by skin drag. The skin drag is small in value for aerofoil. So, the aerofoil has the lowest drag coefficient at that Reynolds number.

The drag coefficients for the circular cylinders in tandem arrangement are listed in Tables 8, 9 and 10 for different flow speeds and L/D ratios.

From Table 8 and Figure 5, for L/D = 2.0, it is seen that, as speed increases, the C_d value of the first cylinder decreases, but for the second cylinder it increases. There is an intersection between the two graphs where the drag

coefficients of the two cylinders are theoretically equal. The speed at the intersection point is approximately 6.5 knots.

Table 8.C_d at L/D = 2.0

L/D = 2.0		
V(knots)	**C_{d1}**	**C_{d2}**
2.5	0.199	0.101
5	0.156	0.129
7.5	0.132	0.146
10.5	0.115	0.157

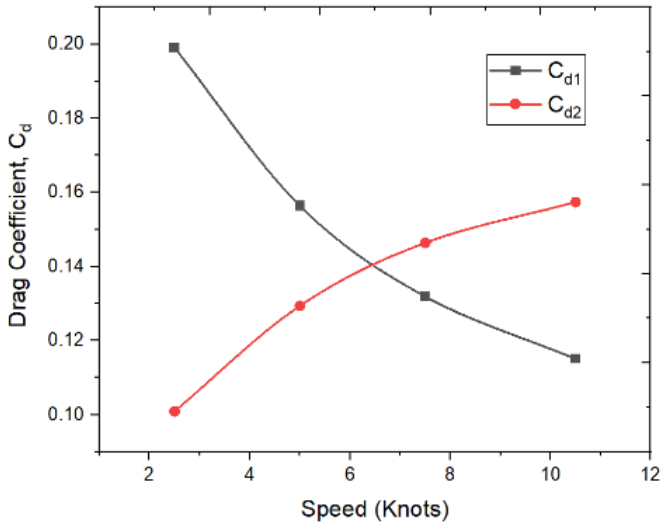

Fig. 5: Drag coefficient vs speed at L/D = 2.0

As the speed increases, the pressure difference between the front and back of the cylinder decreases for the first cylinder. As the cylinder is a bluff body, pressure drag dominates over skin friction drag. So as the pressure difference decreases, the drag coefficient for the first cylinder decreases as well. For the second cylinder, the pressure difference between the front and back of the cylinder increases with speed. So, the pressure drag and the drag coefficient increase. Alternatively, as the speed increases for the first cylinder, the separation point of the flow moves further downstream. As the flow separation is delayed, the wake size also decreases, and wake becomes narrower. Pressure loss is less due to less energy loss in wake. As a result, the pressure difference between the front and back of the cylinder reduces, lowering pressure drag and thus overall drag. For the second cylinder, as the speed increases, the drag coefficient also increases. This is because, as the speed increases, the disturbance on the second cylinder from the first cylinder also increases, and hence the pressure difference between the front and back of the cylinder increases and the drag coefficient increases.

Table 9. C_d at L/D = 2.5

L/D = 2.5		
V(knots)	**C_{d1}**	**C_{d2}**
2.5	0.199	0.158
5	0.159	0.183
7.5	0.136	0.199
10.5	0.121	0.209

From Table 9 and Figure 6, for L/D = 2.5, the trend is the same as for L/D = 2.0. As the speed increases, the C_d value of the first cylinder decreases, but for the second cylinder it increases. The intersection point of the two

curves moves to the left from that for L/D = 2.0. The speed at the intersection point is approximately 4 knots. The rationale for the drag coefficient trend for L/D = 2.5 is the same as it is for L/D = 2.0.

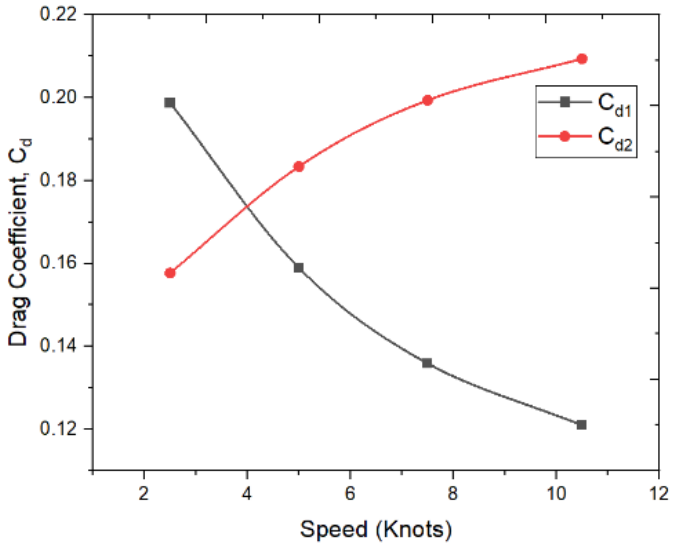

Fig. 6: Drag coefficient vs speed at L/D = 2.5

Table 10. C_d at L/D = 3.0

L/D = 3		
V(knots)	**C_{d1}**	**C_{d2}**
2.5	0.201	0.218
5	0.165	0.240
7.5	0.144	0.253
10.5	0.130	0.261

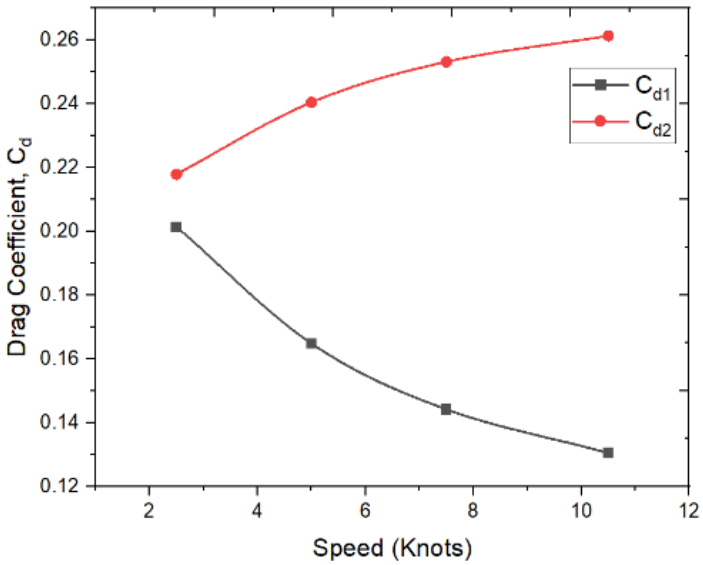

Fig. 7: Drag coefficient vs speed at L/D = 3.0

In Table 10 and Figure 7, for L/D = 3.0, the trend is the same as for L/D = 2 and L/D = 2.5. There is still no intersection point between the curves. If the analysis is done at lower speeds than 2.5 knots, the intersection point will occur at a lower speed than that for L/D = 2.0 and 2.5.

6. Conclusion

From the result and discussion, it can be concluded that, for the single cylinders with the same cross-sectional area at Reynolds number = 1000, the elliptical cylinder with a major axis perpendicular to the flow, i.e., that of vertical orientation, has the highest drag coefficient among the bluff bodies. The elliptical cylinder with a major axis along the flow has less drag due to its more streamline shape than the vertical one. The circular cylinder has a drag coefficient in between these two orientations. For two circular cylinders with a tandem arrangement, the drag coefficient of the first cylinder decreases with the increase in speed, and for the second cylinder, the drag coefficient increases with the increase in speed. The speed at which the drag coefficients of the two cylinders are theoretically equal, decreases as the spacing ratio increases. The study of single cylinders can aid in the development of more acceptable shapes that reduce drag compared to other shapes at the same flow speed, using the same cross-sectional area. Tandem cylinder research can help with future research with more than two cylinders in tandem. For example, in a pile of several cylinders, the exterior flow around these cylinders can be studied using current research knowledge. The study offers more development potential in the three-dimensional analysis. The pressure distribution along the vertical direction can be determined in 3-D analysis, whereas only the in-plane distribution of pressure can be determined in 2-D analysis. The effect of the wave on the cylinders can be explored in 3-D analysis. In 2-D analysis, the influence of the bottom is ignored. However, in 3-D analysis, the bottom and free surface effects can be considered as well. After considering the above features, the study can be further improved.

References

Achenbach, E. (1968). Distribution of local pressure and skin friction around a circular cylinder in crossflow up to Re= 5× 106. Journal of Fluid Mechanics, 34(4), 625-639. https://doi.org/10.1017/S0022112068002120

Biermann and Herrnstein (1933). The interaction between struts in various combinations. Nat. Adv. Comm. Aer. Tech. Rep, 468.

Bokaian, A., and Geoola, F. (1984). Wake-induced galloping of two interfering circular cylinders. Journal of Fluid Mechanics, 146, 383-415. https://doi.org/10.1017/S0022112084001920

Derakhshandeh, J. F., and Alam, M. M. (2020). Reynolds number effect on the flow past two tandem cylinders. Wind and Structures, 30(5), 475-483. https://doi.org/10.12989/was.2020.30.5.475

Hu, X., Zhang, X., and You, Y. (2019). On the flow around two circular cylinders in tandem arrangement at high Reynolds numbers. Ocean Engineering, 189, 106301. https://doi.org/10.1016/j.oceaneng.2019.106301

Igarashi, T. (1981). Characteristics of the flow around two circular cylinders arranged in tandem: 1st report. Bulletin of JSME, 24(188), 323-331. https://doi.org/10.1299/jsme1958.24.323

Ishigai, S., Nishikawa, E., Nishimura, K., and Cho, K. (1972). Experimental study on structure of gas flow in tube banks with tube axes normal to flow: Part 1, Karman vortex flow from two tubes at various spacings. Bulletin of JSME, 15(86), 949-956. https://doi.org/10.1299/jsme1958.15.949

King, R. and Johns, D. J. (1976). Wake interaction experiments with two flexible circular cylinders in flowing water. Journal of Sound and Vibration, 45(2), 259-283. https://doi.org/10.1016/0022-460X(76)90601-5

Kitagawa, T. and Ohta, H. (2008). Numerical investigation on flow around circular cylinders in tandem arrangement at a subcritical Reynolds number. Journal of Fluids and Structures, 24(5), 680-699. https://doi.org/10.1016/j.jfluidstructs.2007.10.010

Ljungkrona, L., Norberg, C. H., and Sunden, B. (1991). Free-stream turbulence and tube spacing effects on surface pressure fluctuations for two tubes in an in-line arrangement. Journal of Fluids and Structures, 5(6), 701-727. https://doi.org/10.1016/0889-9746(91)90364-U

Mahmud, I. H., Pal, P. K., Rahman, A., and Yunus, A. (2018). A study on seasonal variation of hydrodynamic parameters of Padma River. Journal of Modern Science and Technology, 5(1), 1-10.

Oka, S., Kostic, Z. G., and Sikmanovic, S. (1972, August). Investigation of the heat transfer processes in two cylinders in cross flow. In International Seminar on Recent Development in Heat Exchangers. https://doi.org/10.1016/0017-9310(72)90075-0

Okajima, A. (1979). Flows around two tandem circular cylinders at very high Reynolds numbers. Bulletin of JSME, 22(166), 504-511. https://doi.org/10.1299/jsme1958.22.504

Pannell, J. R., Griffiths, E. A., and Coales, J. D. (1915). Experiments on the interference between pairs of aeroplane wires of circular and lenticular cross section. Reports and Memoranda-Aeronautical Research Council (Great Britain), Report, 208.

Rahman, M. M., Karim, M. M., and Alim, M. A. (2007). Numerical investigation of unsteady flow past a circular cylinder using 2-D finite volume method. Journal of Naval Architecture and Marine Engineering, 4(1), 27-42. https://doi.org/10.3329/jname.v4i1.914

Zdravkovich, M. M. (1977). Review of flow interference between two circular cylinders in various arrangements. Journal of Fluids Engineering, 99(4): 618-633. https://doi.org/10.1115/1.3448871